MAGNETIC FIELD IMAGING OF STEEL REINFORCING BARS IN CONCRETE USING PORTABLE SCANNING SYSTEMS

Z.Z. Yu, P.A. Gaydecki, I. Silva., B.T. Fernandes
Department of Instrumentation and Analytical Science
UMIST
PO Box 88
Manchester
M60 1QD
UK

F.M. Burdekin
Department of Civil Engineering
UMIST
PO Box 88
Manchester
M60 1QD
UK

INTRODUCTION

Concrete structures throughout the world face the danger of sudden collapse if the condition of their steel reinforcement is not monitored regularly. Bridges are the most vulnerable to catastrophic failure as they continuously carry dynamic loads. In the United Kingdom, there are more than 150,000 concrete bridges and the annual repair bill is estimated at £500 million. In the United States of America, the situation is even more serious. It was reported in 1977 that more than one in six bridges were unsafe and that it would take more than two centuries to replace the 40,000 deficient structures, given the rate at which funds were currently available [1]. The repair costs for the rest of the world can only be guessed at.

The strength of a concrete bridge structure is governed by the integrity of its steel reinforcement. In most structures, the steel begins to corrode for a number of reasons. It is therefore vitally important to be able to detect the very early stages of corrosion in the reinforcement so that economic remedial action can be taken. Visual inspection only yields results when the steel is corroded to such an extent that spalling of the external concrete cover is evident. Usually at this stage, enough damage has been done to necessitate complete replacement of the bridge section. There are many commercial methods of assessing the condition of bridges but the most convincing method is to actually inspect the steel reinforcement itself. For total assurance, this requires removal of the concrete cover and is therefore destructive in practice. A system that could non-destructively produce a visual representation of the reinforcement within a structure would therefore be a most useful solution.

The project is composed of two major aspects: hardware which includes a sensor, sensor electronics, digitizer and mechanical scanning systems, and software, which includes the data acquisition software, x-y position control and image reconstruction algorithm.

Review of Progress in Quantitative Nondestructive Evaluation, Vol. 18
Edited by Thompson and Chimenti, Kluwer Academic/Plenum Publishers, 1999

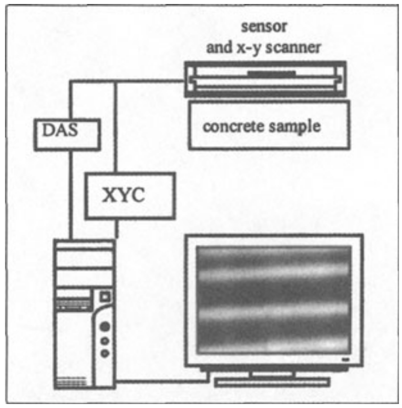

Figure 1. Magnetic field scanner schematic diagram.

Two portable scanning systems are described which produce images of steel reinforcing bars by inductive scanning. The sensing element detects the magnetic field generated by the steel bars due to induced eddy currents and polarisation by excitation coils. At present two different sensors have been developed. The first one is a differential sensor, where an excitation coil is sandwiched between two sensing coils. This configuration nullifies the effect from the excitation field, so that the sensing element responds only to the object field from the steel bars. This sensor also obtains phase information of the object field. The second one uses a heterodyning principle to detect magnetic field changes in the presence of reinforcing bars [2]. Scanned data from both systems are presented. Three image reconstruction algorithms are described. The systems feature new designs of x-y scanner with integrated software enabling an operator to perform a scan sequence, store data, process and display the resulting images from within a single integrated command environment.

THE SYSTEMS

The first system, Mk1, was a laboratory based bench mounted scanner [2]. Two portable systems, Mk2 and Mk3, with two types of sensors have recently been designed and constructed for on site applications. The general layout of the three scanning systems is as shown in Figure 1. Each consists of an x-y scanner with a computerized x-y controller (XYC), a sensor, a data acquisition system (DAS), and a host computer. The host computer controls the x-y positioning system and collects the scanned magnetic field data while the sensor is in motion. The mechanical components have been constructed from non-conductive material, as any metal components would jeopardize the scanning. Although it was impossible to entirely avoid the use of metal, such as motors for scanning, it was decided that they be placed far beyond the sensing area. Cabling and electronic elements also affect the signal by a small amount. They have been carefully arranged to avoid unpredictable effects.

Two types of sensors, a differential sensor and a heterodyning sensor have been developed. Figure 2 shows the photos of the two portable systems Mk2 and Mk3 developed in UMIST, carrying the two types of magnetic field sensors respectively.

MK2 Using a Differential Sensor

The differential sensor consists of two balanced receiving coils and one transmitting coil. The transmitting coil is placed in between the two receiving coils. The two receiving coils are configured in such a way that the induced voltages on them are in opposite phase so that a null condition can be achieved when an excitation field is generated. When steel is within its

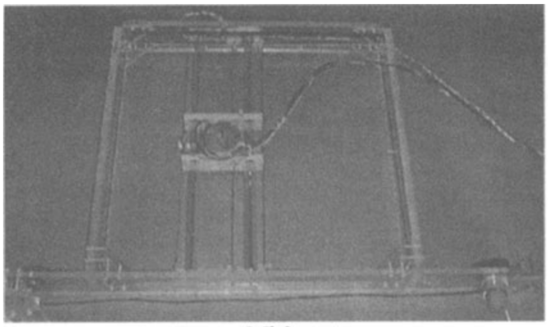

a. Mk2 system

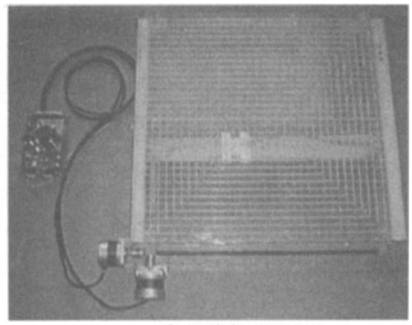

b. Mk3 system

Figure 2. Two portable magnetic field scanning systems developed.

detection range (100mm) the object field will be detected. Since the two receiving coils respond to the difference of the object field on two points, it is called a differential sensor. Figure 3 shows the block diagram of the sensing system. The sensor has a linear response to the object field in terms of its strength and phase. This field, carrying object information, such as the location, size and even the condition of the steel bars, is detected by the receiving coils. Phase sensitive detection is used to resolve real and imaginary components at each scanning point. When the 2D area is scanned, two sets of raw data, real and imaginary, are obtained and post-processed to obtain the image of the bars. Figure 4 shows the plots of real and imaginary components of the scanned data. The scanned concrete has four bars in the y direction and three bars in the x direction. The raw data clearly shows four ridges in the y direction and three in the x direction. From the outline of the ridges, it is deduced that the y direction bars are above the x direction bars. With image reconstruction algorithms, more accurate distribution and the size of the bars are determined.

<u>MK3 Using a Heterodyning Sensor</u>

The heterodyning sensor consists of an inductance coil incorporated into a tuned circuit whose frequency depends on the coil's impedance and inductance. The impedance is itself dependent on the conductivity of the medium through which the lines of flux pass[3]. If it is in the vicinity of a metal, the coil's impedance will change, since eddy currents will be set up within the metal, creating a secondary magnetic field around it. This results in a change in frequency of the tuned circuit. Information about the steel bars is obtained by scanning the sensor across an area of concrete cover. The perturbation is detected by a circuit, which

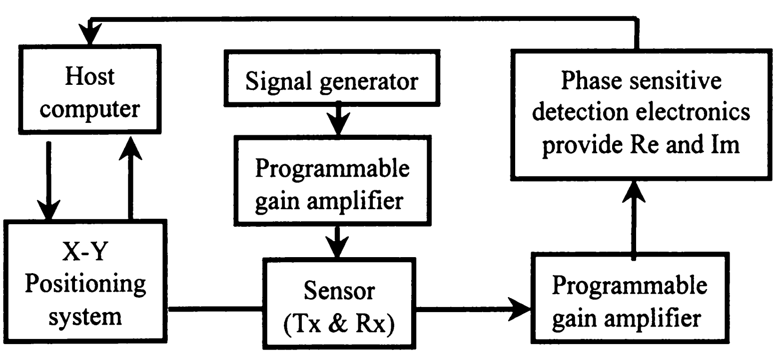

Figure 3. Block diagram of MK2 Magnetic field scanner using a differential sensor.

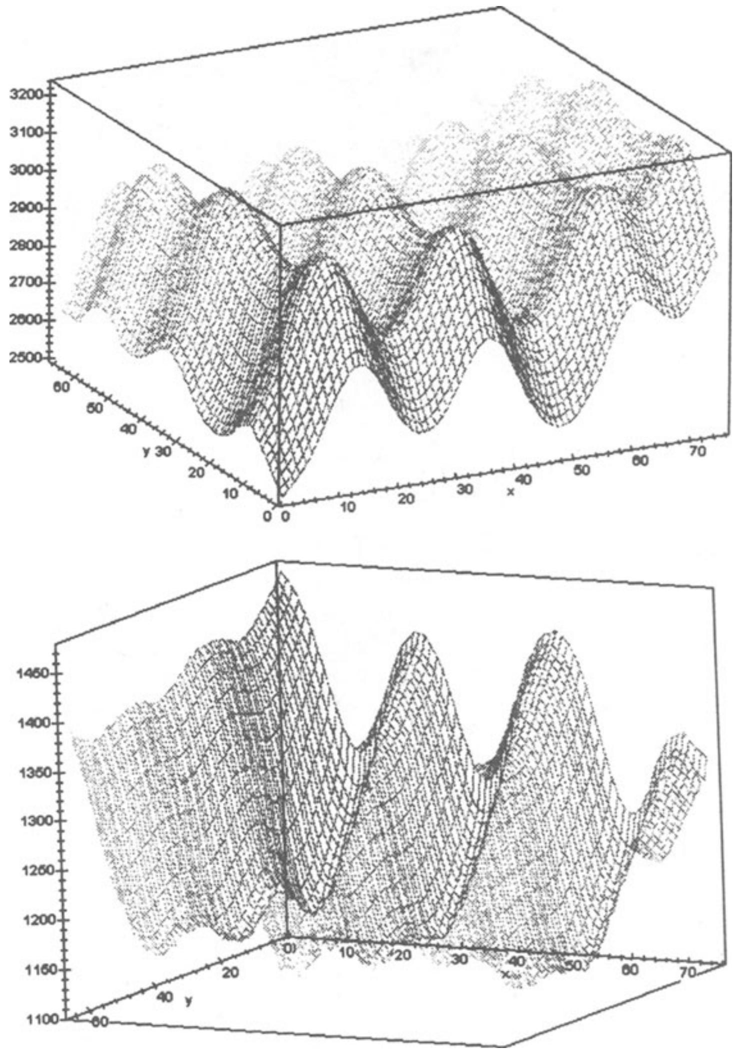

Figure 4. Real (top) and imaginary (bottom) components of scanned data.

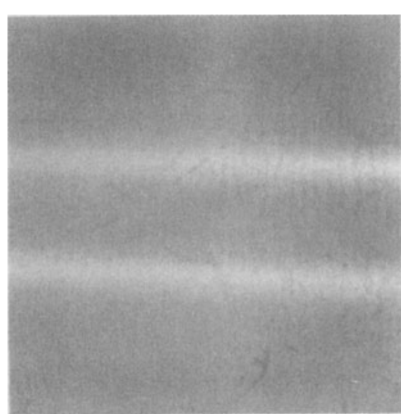

Figure 5. The scanned image of raw data from heterodyning sensor.

compares a stable frequency to that of the tuned circuit and outputs a beat frequency. This beat frequency is converted into a voltage and then input to a computer via an analogue-to-digital converter (ADC) for further processing. More details have been described in [2].

For a typical scan area of 440 mm^2 and the sensor being sampled at every 1.1 mm, the data is stored in word (2 bytes) format for each point, resulting in a maximum file size of 320 kbytes for such a scan. Sample distances and scan dimensions can be altered by the user. The settings chosen have been found to be adequate for analysis.

Raw images are generated on a computer screen for each line scanned. This is done by representing each digital datum as a picture element in a shade of grey. Figure 5 shows a raw image from a 440 mm^2 scanned area.

The software to control the scanner includes a platform for signal acquisition, image display and processing and is written in Borland Delphi 3. The acquisition circuit incorporates a full wave rectifier, an on board PGA allowing gains 1, 10, 100 and 1000, and a 16 bit ADC.

Other Sensors under Development

Two other sensing devices being developed are a Hall effect sensor and an inductive pick-up coil. Hall effect devices can be used to monitor both AC and DC fields producing an output voltage proportional to the strength of the magnetic field passing through them. They can also be incorporated into an array without affecting the responses of each other as coils would by mutual inductance. Inductive sensors can only produce signals from AC magnetic fields but are often more sensitive than Hall effect sensors. They can also be used in tuned circuit arrangements for picking up low signals. In the Hall effect device, an AC magnetic field is used to energize the steel bars embedded within the concrete. The induced field is sensed and an image is obtained by performing a x-y scan of the concrete structure.

IMAGE POST PROCESSING

Various image processing techniques can be used to enhance raw images. Here, three of the methods used in this project are described.

Peak Detection Method

In some instances, it is desirable to be able to have knowledge about the general contents of the area scanned. The number of bars, their relative orientations and their dimensions are some of the important factors. A simple but effective peak detection method has been developed by the authors for this purpose. Using this technique, objects normally undetectable by observing the raw image data have been located.

Figure 5 is a raw image of three bars. Two are placed horizontally and the third is placed 10mm under and perpendicular to the other two. The area scanned was 440 mm^2 sampled in 1.1 mm steps. The sensor was positioned 30mm above the upper bars. In this image, the vertical bar cannot easily be discerned by visual inspection.

The algorithm determines the peaks in the profile by differentiation. First, the raw signal image, $I_0[x,y]$, is averaged as $I_1[x,y]$, or smoothed using Bezier splines to minimise random noise effects [4]. It is then differentiated by subtracting adjacent values in each line:

$$I_1[n] = I_1[n+1] - I_1[n] \tag{1}$$

The maximum values of the differentiated signal are then obtained by examining the gradients on either side of the current datum in the array to find a maximum. To visually represent this finding in the image, its value is set to 256, which is a bright pixel. The above

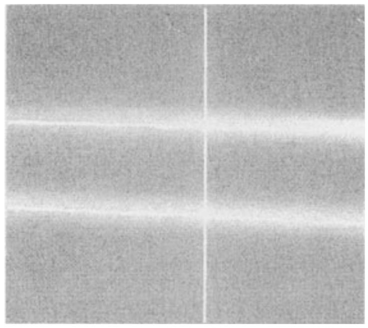

Figure 6. The processed image.

process is repeated using vertical scan lines to detect horizontal bars. Depending on the raw data's signal to noise ratio, further filtering may be necessary to remove the image noise. Clustering and line drawing algorithms are also being used to represent the bars clearly [5]. In total, the computation time is 15 seconds for a 640 X 480 pixel image using a computer with a P150 central processor and 16 Megabytes of memory. Figure 6 shows the results obtained by processing Figure 5. Both horizontal and the vertical bars have been successfully detected.

Neural Networks Method

Another method that is being tested at present uses neural networks to enhance images of steel bars. Neural networks are potentially function approximators and recent applications include image processing, spectral estimation and signal compression [6] and [7]. The algorithm presented is applied to images obtained from inductive scanning to approximate a non-linear function, which can be a very spread representation of the actual image. The converging method uses the neural network energy minimisation. Consider an image $Y(x,y)$ represented by the model:

$$Y(x,y) = A[H(x,y) * X(x,y) + N(x,y)] \tag{2}$$

where A is the system amplification factor, $H(x,y)$ is the point spread function of the sensing system, $X(x,y)$ is the original image and $N(x,y)$ is the noise added in the scanning process, independent of the x and y co-ordinates but dependent on the image signal magnitude X. An energy function E is defined by:

$$E = Y(x,y) - A[H(x,y) * X(x,y)] \tag{3}$$

If we also define a G objective function as:

$$G(X) = -\sum_{j=1}^{N} \ln(x_j) \tag{4}$$

and a penalty function by:

$$P_i(X) = (0.5(\sum_{j=1}^{N} H_{ij} x_j - y_i))^2 \tag{5}$$

where i and j subscripts represent the image dimension, i referring to the output and j to the input images respectively, N is the number of pixels in the image. We can then define a neural

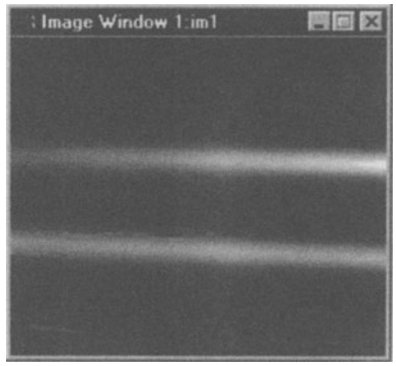

Figure 7. Neural network image processing result.

network energy function by:

$$NNE(t) = -G(X(t)) + K\sum_{i=1}^{M} P_i(X(t)) \tag{6}$$

where K is a constant. Equation (7)'s first derivative is given by:

$$\frac{d(NNE(t))}{dt} = \sum_{i=1}^{M}\left(-\frac{\partial G}{\partial t} + K\sum_{j=1}^{N}\frac{\partial P}{\partial t}\right)\frac{dx_i}{dt} \tag{7}$$

The proposed algorithm has then two layers of neurons containing the partial differentials of G and P. The connection strength of the network H_{ij} is also time variable and is updated by the expression:

$$H_{ij} = H_{ij} + \frac{\partial P / \partial t}{dx / dt}\alpha \tag{8}$$

where $0<\alpha<1$ and is a learning constant. Equation (8) states that the time variation of NNE is a function of space and it approaches a minimum at a certain point. At this point, the image signal X can be reconstructed.

Figure 7 shows the results of applying the neural network algorithm to Figure 5. The processed image is enhanced. There is, however, some noise due to local minimum problems in the algorithm approach. Another problem with this method is that it needs large amount of computer resources, as the connection strengths have dimension of L^2, L being the image size, therefore requiring large images to be split into small images and treated separately. This procedure aggravates the noise problem. The complete procedure took 5 minutes to process this 400 x 400 pixel image. This was accomplished by processing sub-images of 30 x 30 pixels.

Analytical Method for Imaging Electrical Current

This is a relatively new concept for imaging objects which has been proven possible with recent results showing a promising future. [8]. The basic idea is that the magnetic field is only linked with electrical current. For steel bars, virtual current, including eddy current and polarisation current, can be imagined to flow within the body of the target. This current generates the object field being scanned. If the current position were known, the object size and position would be the same. In the one dimensional case, suppose $B_{x(arb)}(x)$ is the arbitrary magnetic field in X-direction generated by arbitrary currents $I(x)$ flowing in a single infinitely long straight conductor in the Y-direction. The current position and values are given by

$$I(x) = \frac{1}{\pi^2 \mu^2} \int_{-\infty}^{\infty} \int_{-\infty}^{\infty} B_{x(\mathrm{arb})}(x) e^{-jxu} dx e^{|u| + jux} du \tag{9}$$

where μ is the permeability of the medium, u is the spatial frequency term. Theoretically, reconstructed steel bar images can be obtained by deconvolution methods. In practice, signal to noise ratio and the area of the scan limit image quality.

CONCLUSION

Two complete systems comprising inductive sensors, novel all-plastic mechanical x-y scanner and totally integrated software have proven very effective in imaging steel bars. The sensors are being optimised for sensitivity and scanning speed. The bar detection algorithms are still at the embryonic stage of development but the results obtained thus far are very promising. The neural network algorithm results are equally satisfying. The development of an integrated system for on-site testing is a realistic prospect within the next twelve months.

ACKNOWLEDGEMENT

The authors gratefully acknowledge the Engineering and Physical Science Research Council of UK for financially supporting this work.

REFERENCES

1. G.P. Mallett, State-of-the-art review, repair of concrete bridges, Thomas Telford Services Ltd. (1994).
2. P. A. Gaydecki, F.M. Burdekin, *An inductive scanning system for two dimensional imaging of reinforcing components in concrete structures*, Meas. Sci. Technol. 5 1272-1280, UK. (1994)
3. G.R. Hugo and S.K. Burke, (1988), *Impedance changes in a coil due to a nearby small conducting sphere*, J. Phys. D: Appl. Phys. 21 33-38, UK.
4. E.I. Okanla and P. A. Gaydecki, (1996), *A real-time audio frequency cubic spline interpolator*, Signal Processing, Vol 49, pp 45 – 55.
5. R.C Gonzalez, P. Wintz, (1987) *Digital Image Processing*, Second Edition, Addiso-Wesley Publishing Company.
6. F. Luo and R. Unbehauen, *Applied Neural Networks for Signal Processing*, Cambridge University Press, 369p., 1997.
7. B. Kosko, Neural Networks for Signal Processing, Prentice Hall, 399p., 1992.
8. Z. Z. Yu and P. A. Gaydecki, *One dimensional current imaging based on an analytical solution of magnetic field distribution: applications to non-destructive testing of reinforcing bars in concrete*. Meas. Sci. Technol. Vol. 9 No. 9 Sept 1998.